A Study on High-Efficiency Energy Detection-Based Spectrum Measurements

Hiroki Iwata*§, Kenta Umebayashi*, Ahmed Al-Tahmeesschi*, Satya Joshi‡,
Miguel López-Benítez† and Janne J Lehtomäki‡
*Dept. of Electrical and Electronic Engineering, Tokyo University of Agriculture and Technology, Japan
†Dept. of Electrical Engineering and Electronics, University of Liverpool, United Kingdom
ARIES Research Centre, Antonio de Nebrija University, Spain
‡Centre for Wireless Communications, University of Oulu
Email: §hiroki_iwata@ieee.org

Abstract—**Statistical information in terms of spectrum occupancy is useful for the efficient and smart dynamic spectrum sharing, and it can be obtained by long-term, broadband, and wide-area spectrum measurements. In this paper, we investigate an energy detection (ED)-based spectrum measurements, in which the noise floor (NF) estimation is a key functionality for the appropriate ED threshold setting. Typically, the NF has the slowly time-varying property and frequency-dependency, and several NF estimation algorithms including forward consecutive mean excision (FCME) algorithm-based method have been proposed. However, these methods did not deeply consider the slowly time-varying property of the NF and are computationally inefficient. Accordingly, we propose a computational complexity reduction algorithm based on NF level change detection. This algorithm is computationally efficient, since it skips the NF estimation process when the NF does not change. In numerical evaluations, we show the efficiency and the validity of the proposed algorithm.**

I. Introduction

Dynamic spectrum access (DSA) aims to solve the spectrum scarcity problem by increasing spectrum utilization [1]. This can be achieved by allowing unlicened users (secondary users: SUs) to access the spectrum of licensed incumbent user (primary users: PUs) in an opportunistic and non-interfering manner during PU idle times (spectrum holes). In order to effciently share spectrum between PUs and SUs, it is required to sense the spectrum (spectrum sensing) and then manage wireless resources (e.g., bandwidth, transmit power, etc.). The requirements of the spectrum sensing, such as accuracy, latency and implementation cost are substantially demanding [2], [3]. On the other hand, in the wireless resource management, it is required to manage wireless resources so that SUs do not cause any harmul interference to PUs and increase spectrum utilization efficiency.

In order to resolve the issue of spectrum sensing and provide the efficient wireless resource management, an advanced DSA approach (known as smart spectrum access (SSA)) has been investigated [4], [5]. SSA exploits prior information in terms of PUs' spectrum usage, and this information is obtained by long-term, broadband and wide area spectrum measurements. In fact, by the use of SSA approach, it has been shown that channel occupancy rate (COR) information can enhance spectrum sensing performance [6], [7]. It can also enhance spectrum management, channel selection and MAC protocol [8], [9].

In this paper, we focus on the spectrum measurement part for realizing SSA. In general, the spectrum measurement consists of acquisition of the data associated with spectrum usage (e.g., I/Q data, power data) and processing the obtained data such as spectrum analysis, spectrum usage detection and estimation of statistical information such as COR. Actually, there have been many spectrum measurement campaigns (see [10], [11] and references therein), and almost all the campaigns utilize energy detector (ED) as a spectrun usage detection technique.

One key challenge for the ED is the detection threshold setting since the threshold highly affects the detection performance. Therefore, there are sevelal threshold setting criteria including the m-dB criterion and the constant false alarm rate (CFAR) criterion [12]. Basically, we need an accurate noise floor (NF) information no matter what criteria we adopt to set the threshold satisfying an adopted criterion.

Most of the previous spectrum usage measurements utilizing ED have exploited a fixed NF information, which is obtained by switching the receiver input to a matched load or is measured in an anechoic chamber before starting the measurements [13]. These measurements implicitly assume that the NF does not change with time. However, the NF should be estimated regularly due to its time dependency [14]. Moreover, the NF has equipment-specific frequency dependency [15], [16]. Therefore, several NF estimation methods have been investigated. In [17], the NF estimation method applying forward consecutive mean excision (FCME) algorithm is proposed. The method can estimate the NF accurately in the presence of PU signals if the measured data such as I/Q data partially contain noise samples and the noise samples are white. Thus, this method does not work if the NF has the frequency dependency (i.e., non white noise). In [16], an NF estimation considering the frequency dependency of the NF was proposed. The method [16] has exploited the FCME algorithm twice in two-dimensional directions, i.e., time and frequency. These FCME-based methods can attain accurate NF estimation performance at the cost of slightly high computational cost, as the FCME algorithm exploits sorting algorithm and these methods are
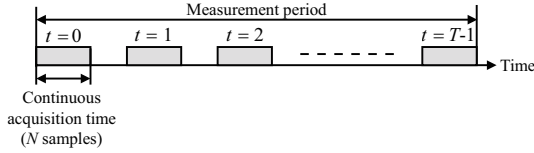
Fig. 1.   The configuration of time frames in measurement process
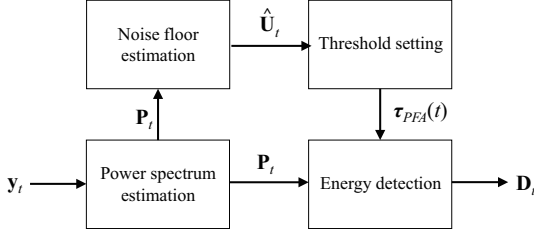

Fig. 2.   General signal processing model for spectrum measurement

performed independently regardless of the time variation of the NF. However the NF may not change for several tens of minites [14]. This fact motivates us to propose a new method where the NF is estimated only when it actually changes.

This paper investigates efficient ED-based spectrum measurements. The proposed method performs the NF estimation only when there is a change in the NF. The main contributions of this paper are as follows:

- We propose an NF level change detection method to decide whether the NF estimation can be skiped or not. The method is based on the ED result with detection threshold based on previous NF estimate. Thus, the NF estimation process is skipped when the previous detection threshold is decided to be adequate, achieving efficient ED-based spectrum measurements.
- The proposed method has lower computational complexity of the NF estimation while it offers the comparable NF estimation performance with respect to the existing high-performance NF estimation methods such as FCME algorithm-based method. We numerically verify it.

The rest of the paper is organized as follows: Section II is devoted to the description of spectrum usage measurement methodology, the time variation model of NF level and the significance of our work. In Section III, we introduce the efficient ED-based measurements withe the NF level change detection. The numerical evaluation and its corresponding discussion are provided in Section IV. Finally, Section V concludes our paper.

II. SYSTEM MODEL

We assume that a spectrum sensor such as real-time spectrum analyser or software-defined radio which can acquire I/Q samples, and we focus on the processing of the acquired I/Q samples.

Configuration of time frames for the spectrum measurement is shown in Fig. 1. The spectrum measurement is long-term (e.g., from several days to several months) specified by the measurement period. The measurement period consists of T measurement period. The measurement period consists of T

times continuous data acquisition period. One continuous data acquisition period consists of N I/Q baseband samples, and we index a data acquisition period by t, $t \in \{0, 1, \cdots, T-1\}$.

The general signal processing used for spectrum measurement is shown in Fig. 2. The first step is the power spectrum estimation with Welch FFT [18] using I/Q baseband samples $\mathbf{y}_t$. Then, the NF estimation is performed and we denote the estimated NF as $\hat{\mathbf{U}}_t$. Conventionally, the NF estimation based on the estimated power spectrum is performed once per a continous data acquisition period. But our proposed algorithm can skip the NF estimation procedure and use the estimated NF at the previous data acquisition time $t-1$, if the change in the NF is not detected. In Sect. III, we will explain the proposed algorithm in detail. After the NF estimation, the threshold setting for ED is performed using $\hat{\mathbf{U}}_t$. Finally, the ED with the set threshold $\boldsymbol{\tau}_{P_{FA}}(t)$ is performed to obtain the spectrum usage decisions $\mathbf{D}_t$. Below is the more detailed explanation for the process.

Let us focus on the tth data acquisition time ($t \in \{0, 1, \cdots, T-1\}$). At first, the acquired I/Q baseband signal $\mathbf{y}_t = [y_t[0], y_t[2], \cdots, y_t[N-1]]^T$ is divided into K Welch FFT blocks with N_s samples. Thus, the I/Q baseband signal $\mathbf{y}_k^{(t)}$, $k \in \{0, 1, \cdots, K-1\}$ in the kth Welch FFT block is given by $\mathbf{y}_k^{(t)} = [y_t[kN_s + 1], \cdots, y_t[kN_s + N_s]]^T$.

The power spectrum estimation with Welch FFT consists of three steps: segmentation of $\mathbf{y}_k^{(t)}$ with a specific FFT size and an overlap ratio, calculation of multiple power spectra, and averaging of the power spectra [18]. The I/Q baseband signal $\mathbf{y}_{k,l}^{(t)}$, $l \in \{0, 1, \cdots, L-1\}$ at lth segment and kth Welch FFT block is given by

$$\mathbf{y}_{k,l}^{(t)} = y_t[kl(1-\rho)N_{FFT}+1], \cdots, y_t[kl(1-\rho)N_{FFT}+N_{FFT}]]^T. \quad (1)$$

where N_{FFT} and $\rho \in [0, 1)$ indicate the FFT size and the overlap ratio between the adjacent segments, respectively. In the rest of the paper, we assume that $\rho = 0.5$ because it has been confirmed to be appropriate choice for good signal detection performance [19]. Moreover, N_s and N_{FFT} are assumed to be powers of two. In this case, the number of segments L is given by $L = 2N_s/N_{FFT} - 1$.

After the segmentation, normal FFT is performed with respect to each segment. The result of FFT operation of $\mathbf{y}_{k,l}^{(t)}$ is given by

$$\mathbf{Y}_{k,l}^{(t)} = \frac{1}{\sqrt{N_{FFT}}} \mathbf{F} \mathbf{W} \mathbf{y}_{k,l}^{(t)} \quad (2)$$

where $\mathbf{F} = (\exp(-j2\pi mf/N_{FFT}))_{m,f=0,1,\cdots, N_{FFT}-1}$ is the discrete Fourier transform matrix. The diagonal matrix $\mathbf{W} = \mathrm{diag}(w_0, w_1, \cdots, w_{N_{FFT}-1})$ is a matrix where its diagonal elements are coefficients w_m of the utilized FFT window with $\sum_{m=0}^{N_{FFT}-1} w_m^2 = 1$. Here, we use Hamming window as it has been shown that it can achieve slightly better performance compared to other window functions in [17].

Finally, the calculated power spectra are averaged. Thus, the averaged power spectrum estimate $\mathbf{P}_k^{(t)}$ at kth Welch FFT
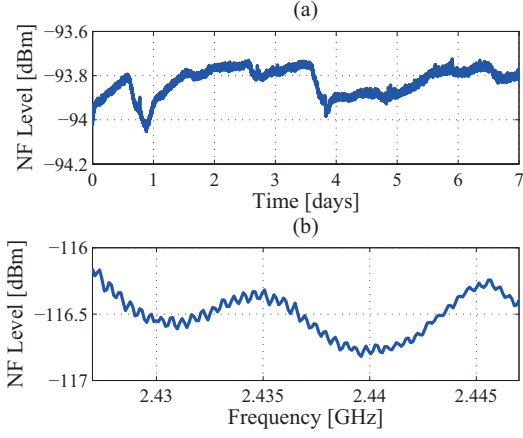
Fig. 3. NF measurement ((a) NF level evolution, (b) Power spectrum of NF)

Fig. 4. Obtained false alram rate as a function of NF level variation factor

block is given by

$$\mathbf{P}_k^{(t)} = \frac{1}{L} \sum_{l=0}^{L-1} |Y_k^{(t)}[l,f]|^2$$
$$= [P_k^{(t)}[0], \cdots, P_k^{(t)}[f], \cdots, P_k^{(t)}[N_{FFT}-1]]^T, \quad (3)$$

where $f = 0, 1, \cdots, N_{FFT}-1$ indicates the index number of frequency bin. We define a matrix $\mathbf{P}_t = [\mathbf{P}_1^{(t)} \mathbf{P}_2^{(t)} \cdots \mathbf{P}_K^{(t)}]$.

The ED result at the kth Welch FFT block and the fth frequency bin is obtained as

$$D_t[k,f] = \begin{cases} 1 \ (P_k^{(t)}[f] > \tau_{P_{FA}}[f](t)) \\ 0 \ (\text{otherwise}), \end{cases} \quad (4)$$

where 1 and 0 correspond to the decisions of occupied spectrum ($\mathcal{H}_1$) and vacant spectrum ($\mathcal{H}_0$), respectively. The occupied spectrum ($\mathcal{H}_1$) indicates that PU signal exists in the frequency bin partially or completely and vacant spectrum ($\mathcal{H}_0$) indicates otherwise (no signal present). The detection threshold $\tau_{P_{FA}}(t)$ is set based on NF estimate $\hat{\mathbf{U}}_t = [\hat{U}[t,0], \hat{U}[t,1], \cdots, \hat{U}[t,f], \cdots, \hat{U}[t,N_{FFT}-1]]^T$ so that $\tau_{P_{FA}}(t)$ satisfies CFAR criterion.

A. Time Variation Model of Noise Floor Level

Figure 3 shows (a) the NF level evolution for one week (01/12/2018–07/12/2018) and (b) the power spectrum of the NF. This result was measured at our laboratory in Koganei campus, Tokyo University of Agriculture and Technology, Tokyo, Japan. The spectrum sensor used was a real-time spectrum analyzer (Tektronix RSA306B). The result was obtained every one minute by switching the sensor input to a matched load. Figure 3 (a) verifies that the NF level slowly changes with time between around -94.05dBm and -93.72dBm. On the other hand, Fig. 3 (b) shows that the NF has the frequency-dependency. These facts indicate that we should estimate the NF considering the time-varying property and the frequency-dependency of the NF.
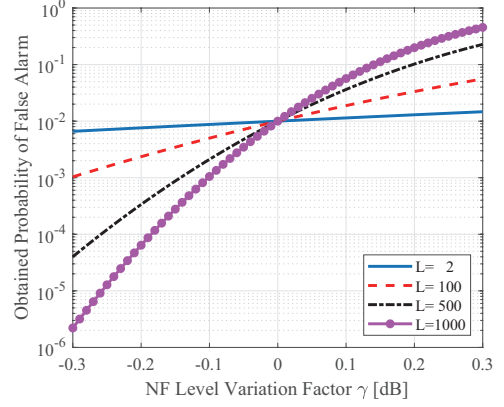
In this work, we model the NF level variation in time

according to the following relationship [16]

$$U[j,f] = \gamma_j \mu_{ref}[f], \quad (5)$$

where γ_j and $\mu_{ref}[f]$ indicate the NF level variation factor and the NF at a reference time instant $j = t_{ref}$ denoted by the reference NF, respectively. This relationship means that the NFs between the reference time instant, and any data acquisition times $j = t$ does not depend on frequency and its variation is multiplicative. To obtain the reference NF, we assume the spectrum sensor has a radio frequency (RF) terminator. The reference NF $\mu_{ref}[f]$ is calculated by time averaging of noise power spectra, and it is given by

$$\mu_{ref}[f] = \frac{1}{M} \sum_{m=0}^{M-1} P_{m,ref}[f], \quad (6)$$

where M and $P_{m,ref}[f]$ indicate the number of time averaging and noise power spectrum, respectively. Furthermore, we assume the NF at least do not change during one data acquisition time.

B. Significance of our work

In this section, we show the significance of our work even slight changes of the NF (e.g., the order of 0.4dBm in Fig. 3 (a)). Thus, we evaluate the the acutally obtained false alarm rate when the threshold $\tau_{P_{FA}}$ is set without considering the change of NF level, i.e., assuming the NF $U[t,f] = \mu_{ref}[f]$ regardless of the time t. The obtained false alarm rate can be calculated as follows [16]

$$P_{FA} = \text{Prob}(P_k^{(t)}[f] > \tau_{P_{FA}}|\mathcal{H}_0) = \tilde{\Gamma}\left(L, \frac{\tau_{P_{FA}}}{\gamma_t \mu_{ref}[f]/L}\right), \quad (7)$$

where $\tilde{\Gamma}(\alpha, \theta)$ indicates a normalized incomplete Gamma function The threshold $\tau_{P_{FA}}$ is set based on CFAR criterion and is given by [16]

$$\tau_{P_{FA}}[f] = \frac{\mu_{ref}[f]}{L} \tilde{\Gamma}^{-1}\left(L, \dot{P}_{FA}\right), \quad (8)$$

where $\dot{P}_{FA}$ is a given target false alarm rate and $\tilde{\Gamma}^{-1}$ indicates the inverse of a normalized incomplete Gamma function. In
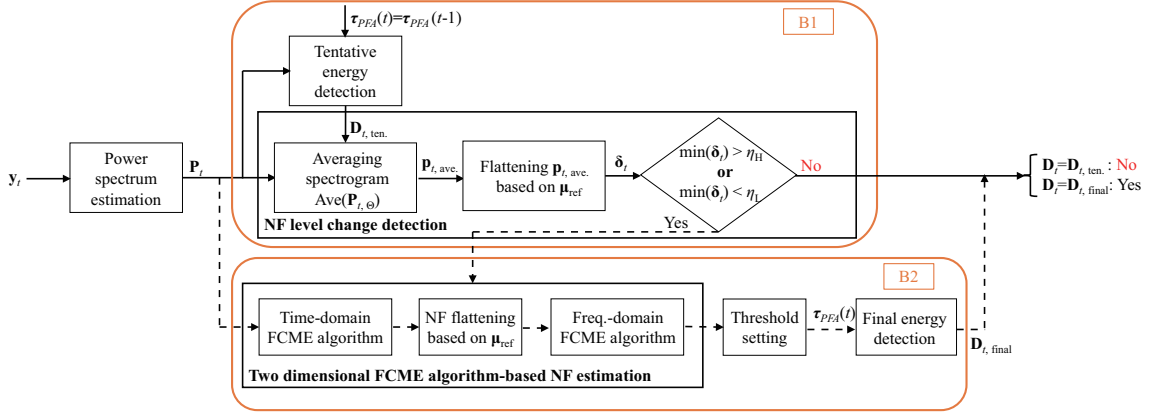
Fig. 5. Block diagram of the proposed ED-based measurement signal processing

Fig. 4, the target false alarm rate $\dot{P}_{FA} = 0.01$. The figure shows, for example, the obtained false alarm rate is about 0.45 in the case of $L = 1000$ and $\gamma = 0.3$dB. That means we should estimate the NF while following slight changes in the NF (say, $\gamma = 0.3$dB).

III. PROPOSED ED-BASED MEASUREMENT SIGNAL PROCESSING

Block diagram of proposed algorithm for spectrum measurement is shown in Fig. 5. There are two blocks: Block 1 (B1) and Block 2 (B2). The process in B1 is executed every spectrum measurement except for the first measurement $t = 0$. On the other hand, B2 is only applied when the NF level change is detected or $t = 0$ since the spectrum sensor does not know the NF in the sensor at first. Therefore, the proposed method can reduce the computational cost of NF estimation processes as the NF level changes slowly.

In B2, we exploit the two-dimensional FCME algorithm-based NF estimation as the NF estimation as it can achieve the high-accurate NF estimation performance while considering the frequency-dependency of the NF [16]. However, the proposed method also could be utilized with other NF estimation methods such as [17], [20], [21]. Briefly, the two-dimensional FCME-based NF estimation estimates the NF level variation factor γ_t at time instant t exploiting the reference NF $\mu_{ref}[f]$ and the estimated power spectrum in the time-frequency plane $\mathbf{P}_t$, where the description of the reference NF is provided in Subsect. II-A [16]. More specifically, it locates the noise-only power samples in power spectrum samples $\mathbf{P}_t$ based on the FCME algorithm, flattens the located noise-only power spectra in frequency exploiting $\mu_{ref}[f]$, and estimates γ_t by applying the FCME algorithm again. Then, the resultant NF estimate is $\hat{U}[t, f] = \hat{\gamma}_t \cdot \mu_{ref}[f]$ where $\hat{\gamma}_t$ indicates the estimate of γ_t. After estimating the NF in B2, the ED is performed based on the set threshold with the estimated NF.

On ther other hand, for other spectrum measurements, i.e., $t \in \{1, 2, \cdots, T-1\}$, the processes in B1 are performed at first. It includes the tentative ED with the detection threshold equal to the one in the previous spectrum measurement, i.e., $\tau_{P_{FA}}(t-1)$, and the NF level change detection. If the change

of the NF is detected, the processes in B2 are enforced and the ED result is the final ED result, i.e., $\mathbf{D}_t = \mathbf{D}_{t,final}$. Otherwise, the ED result equals to the tentative ED result ($\mathbf{D}_t = \mathbf{D}_{t,ten.}$), and $\hat{U}[t, f] = \hat{U}[t-1, f]$ and $\boldsymbol{\tau}_{P_{FA}}(t) = \boldsymbol{\tau}_{P_{FA}}(t-1)$.

The NF level change detection in B1 exploits the result of the tentative ED, $\mathbf{D}_{t,ten.}$ and the power spectrum $\mathbf{P}_t$. Let a set $\Theta[f]$ to be a set consiting of the indices of zeros in $\mathbf{D}_{t,ten.}[f]$, i.e., $\Theta[f] = \{k | \mathbf{D}_{t,ten.}[f] = 0\}$, where $\mathbf{D}_{t,ten.}[f]$ indicates the tentative ED result at frequency bin f. Then, we define a value $p_{t,ave.}[f]$ as the average value of a vector $\mathbf{p}_{t,\Theta}[f]$ in time. Specifically, $p_{t,ave.}[f]$ is given by

$$p_{t,ave.}[f] = \frac{1}{|\Theta[f]|} \sum_{k \in \Theta[f]} P_k^{(t)}[f], \qquad (9)$$

where $|\Theta[f]|$ indicates the cardinality of $\Theta[f]$ and $\mathbf{p}_{t,\Theta}[f] = [P_{k \in \Theta[f]}^{(t)}[f]]$. After that, we perform the NF flattening process using the reference NF $\mu_{ref}[f]$ as in the two-dimentional FCME algorithm-based NF estimation. This process is done as

$$\delta_t[f] = \frac{p_{t,ave.}[f]}{\mu_{ref}[f]}. \qquad (10)$$

We can detect the NF level change by the thresholding process against $\delta_t[f]$ since $\delta_t[f]$ is an estimate of γ_t. Specifically, we decide that the NF level change if $\min(\delta_t) > \eta_H$ or $\min(\delta_t) < \eta_L$. Otherwise, i.e., $\min(\delta_t)$ lies in between η_L and η_H, we decide that the NF level does not change. We apply two thresholds, η_L and η_H since the NF level possibly increases and/or decreases. Both thresholds are set based on $\hat{\gamma}_{t-1}$ and two hyperparameters (Δ_L, Δ_H) and these are given by

$$\eta_L = \Delta_L \cdot \hat{\gamma}_{t-1}, \eta_H = \Delta_H \cdot \hat{\gamma}_{t-1} \qquad (11)$$

where the hyperparameters are set so that the target false alarm rate can be guaranteed. We will investigate several methods for hyperparameters setting as our future work.

IV. NUMERICAL EVALUATIONS

In this section, we evaluate the NF estimation performance of the proposed method based on computer simulations.

Table I
PARAMETER SET

Parameter name	Parameter
Welch FFT block size N_s	2^{10}
FFT size N_{FFT}	2^8
$N_{trial} = T$	10260
σ_z^2	-94dBm
SNR [dB]	[-4 10]
Channel occupancy rate	0.5
Measurement bandwidth	20MHz
Center frequency	2.437GHz
Signal bandwidth	20MHz
$\dot{P}_{FA}$	0.01

Fig. 7. Relative error as a function of SNR.

Fig. 6. NF setting in the simulations ((a) Assumed NF evolution, (b) Assumed reference NF)

Fig. 8. Probability of detection as a function of SNR.

As comparative methods, we consider the original FCME algorithm-based NF estimation [17] and the two-dimensional FCME algorithm-based NF estimation [16]. We assume the spectrum measurements of one wireless local area network (WLAN) channel over 2.4GHz industrial, scientific and medical (ISM) band. Common parameters are summarized in Table I. Figure 6 shows (a) the assumed NF variation in time and (b) the assumed reference NF. These correspond to the approximation to the NF by noise measurements as mentioned in Subsec. II-A (Fig. 3). Specifically, we calculated the NF level and the power spectrum of the NF (the reference NF) according to the experimental result of Fig. 3 by means of polynomial approximation.

Figure 7 shows the relative error in terms of NF estimate $\hat{U}[f]$ given by (12) as a function of SNR

$$\text{RE}[\mathbf{U}] = \frac{1}{N_{FFT} \cdot N_{trial}} \frac{|\hat{U}[f] - U[f]|}{U[f]}, \qquad (12)$$

where N_{trial} and N_{FFT} respectively present the numbers the Monte Carlo trials and the frequency bins.

From Fig. 7, we observe that the error performance of the proposed method approximately coincides with the one of the two-dimensional FCME algorithm-based NF estimation.
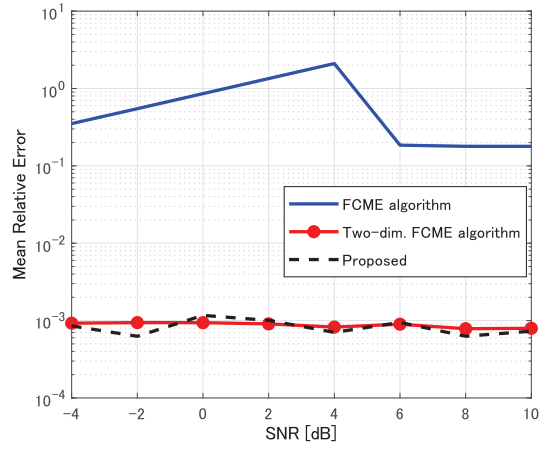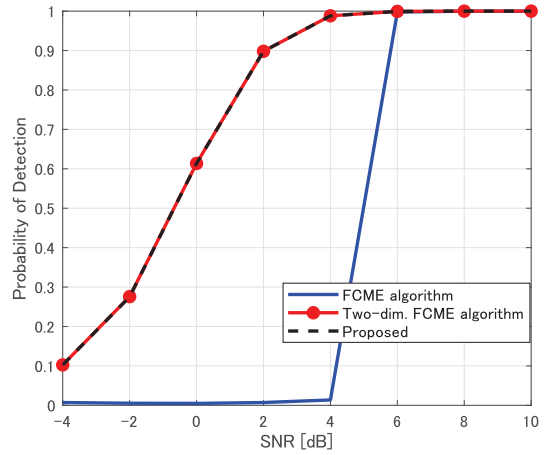
Moreover, the original FCME algorithm-based NF estimation cannot achieve the good NF estimation performance since it does not consider the frequency dependency of the NF.

Figure 8 shows the probabilities of false alarm and detection as a function of SNR, where we set the target probability of false alarm is 0.01. From this figure, the probability of detection of the proposed method almost coincides with the ones of the two-dimensional FCME algorithm-based NF estimation since the proposed method achieves the same NF estimation performance approximately as of the two-dimensional FCME algorithm-based NF estimation as shown in Fig. 7. Again, the detection performance of the FCME algorithm-based NF estimation is not good due to the poor NF estimation performance.

Finally, we evaluate the computational complexity of ED-based measurement with the proposed method or the convetional two-dimensional FCME algorithm-based NF estimation. The complexity of the proposed method is determined by the number of the NF estimations executed $N_{NF,pro.}$, the complexity of the NF level change detection C_{cd}, and the complexity of the NF estimation $C_{NF,two}$, the number of the spectrum measurements T. On the other hand, the complexity of the measurement with the conventional NF
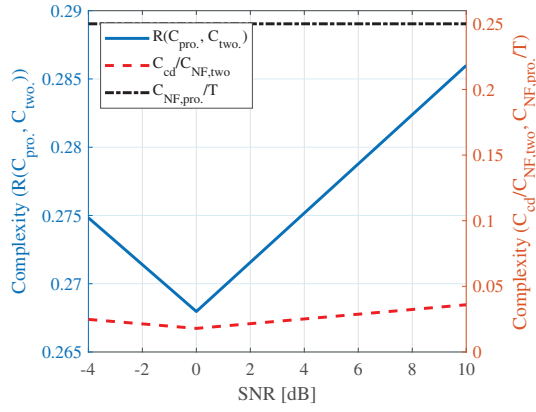
Fig. 9. Computational complexity

estimation is determined by the complexity of the NF estimation $C_{NF,two}$, and the number of the spectrum measurements T. Therefore, we evaluate the ratio of the computational complexity, $R(C_{pro.}, C_{two.})$ between the proposed method-based processing ($C_{pro.}$) and the conventional NF estimation-based processing ($C_{two.}$) given by

$$R(C_{pro.}, C_{two.}) = \frac{C_{pro.}}{C_{two.}} = \frac{C_{cd}}{C_{NF,two}} + \frac{N_{NF,pro.}}{T},$$

where the reduction of the complexity of the proposed method can be achieved if and only if $R(C_{pro.}, C_{two.}) < 1$.

Figure 9 shows $R(C_{pro.}, C_{two.})$ and the proposed method can reduce the complexity by around $1/4$. This reduction is because the number of NF estimation executed is reduced, i.e., $\frac{N_{NF,pro.}}{T} < 1$, and the proposed method has the lower complexity than the conventional method, i.e., $\frac{C_{cd}}{C_{NF,two}} < 1$. Specifically, as shown in Fig. 9, $\frac{N_{NF,pro.}}{T}$ is around 0.25, but $\frac{C_{cd}}{C_{NF,two}}$ is around 0.03. The number of NF estimation executed depends on the changing rate of the NF, so we will evaluate the accuracy and the complexity of the proposed method as our future work.

V. CONCLUSION

In this work, we have proposed an efficient ED-based signal processing for spectrum measurements. We have considered the slowly time-varying property and the frequency dependency of the NF. Specifically, the proposed method can reduce the number of required NF estimations by means of a NF level change detection. Numerical evaluations show that the proposed method enables an accurate spectrum occupancy detection considering the frequency-dependency and slowly time-varying characteristics of the NF, while it reduces the computational complexity.

ACKNOWLEDGMENT

REFERENCES

[1] Q. Zhao and B. M. Sadler, "A survey of dynamic spectrum access," *IEEE Signal Process. Mag.*, vol. 24, no. 3, pp. 79–89, May 2007.

[2] T. Yücek and H. Arslan, "A survey of spectrum sensing algorithms for cognitive radio applications," *IEEE Commun. Surveys Tuts.*, vol. 11, no. 1, pp. 116–130, First quarter 2009.

[3] G. Ding, J. Wang, Q. Wu, Y. Yao, F. Song, and T. A. Tsiftsis, "Cellular-base-station-assisted device-to-device communications in TV white space," *IEEE J. Sel. Areas Commun.*, vol. 34, no. 1, pp. 107–121, Jan. 2016.

[4] K. Umebayashi, K. Moriwaki, R. Mizuchi, H. Iwata, S. Tiiro, J. J. Lehtomäki, M. López-Benítez, and Y. Suzuki, "Simple primary user signal area estimation for spectrum measurement," *IEICE Trans. Commun*, vol. E99-B, no. 8, pp. 523–532, Feb. 2016.

[5] T. Fujii and K. Umebayashi, "Smart spectrum for future wireless world," *IEICE Trans. Commun.*, vol. E100-B, no. 9, pp. 1661–1673, Sep. 2017.

[6] T. Nguyen, B. L. Mark, and Y. Ephraim, "Spectrum sensing using a hidden bivariate Markov model," *IEEE Trans. Wireless Commun.*, vol. 12, no. 9, pp. 4582–4591, Sept. 2013.

[7] K. Umebayashi, K. Hayashi, and J. J. Lehtomäki, "Threshold-setting for spectrum sensing based on statistical information," *IEEE Commun. Lett.*, Apr. 2017.

[8] K. Umebayashi, Y. Suzuki, and J. J. Lehtomäki, "Dynamic selection of CWmin in cognitive radio networks for protecting IEEE 802.11 primary users," in *Proc. IEEE CROWNCOM*, June 2011, pp. 266–270.

[9] Y. Xu, A. Anpalagan, Q. Wu, L. Shen, Z. Gao, and J. Wang, "Decision-theoretic distributed channel selection for opportunistic spectrum access: Strategies, challenges and solutions," *IEEE Commun. Surveys Tuts.*, vol. 15, no. 4, pp. 1689–1713, Fourth quarter 2013.

[10] D. Das and S. Das, "A survey on spectrum occupancy measurement for cognitive radio," *Springer Wireless Pers. Commun.*, vol. 85, no. 4, pp. 2581–2598, 2015.

[11] M. Höyhtyä, A. Mämmelä, M. Eskola, M. Matinmikko, J. Kalliovaara, J. Ojaniemi, J. Suutala, R. Ekman, R. Bacchus, and D. Roberson, "Spectrum occupancy measurements: A survey and use of interference maps," *IEEE Commun. Surveys Tuts*, vol. 18, no. 4, pp. 2386–2414, Fourth quarter 2016.

[12] M. López-Benítez and F. Casadevall, "Methodological aspects of spectrum occupancy evaluation in the context of cognitive radio," *European Trans. Telecommun.*, vol. 21, no. 8, pp. 680 – 693, Dec. 2010.

[13] J. Kokkoniemi and J. Lehtomäki, "Spectrum occupancy measurements and analysis methods on the 2.45 GHz ISM band," in *Proc. EAI CROWNCOM*, Jun. 2012, pp. 285–290.

[14] D. Torrieri, "The radiometer and its practical implementation," in *Proc. IEEE MILCOM*, Oct. 2010, pp. 304–310.

[15] A. Mariani, A. Giorgetti, and M. Chiani, "Robust detection with low-complexity sdrs: A pragmatic approach," in *Proc. IEEE PIMRC*, Sep. 2018, pp. 1–6.

[16] H. Iwata, K. Umebayashi, A. Al-Tahmeesschi, M. López-Benítez, and J. Lehtomäki, "Time and frequency varying noise floor estimation for spectrum usage measurement," in *Proc. IEEE WCNCW*, Apr. 2019.

[17] J. J. Lehtomäki, R. Vuohtoniemi, and K. Umebayashi, "On the measurement of duty cycle and channel occupancy rate," *IEEE J. Sel. Areas Commun.*, vol. 31, no. 11, pp. 2555–2565, Nov. 2013.

[18] P. D. Welch, "The use of fast Fourier transform for the estimation of power spectra: A method based on time averaging over short, modified periodograms," *IEEE Trans. Audio Electroacoust.*, vol. 15, no. 2, pp. 70–73, June 1967.

[19] H. Iwata, K. Umebayashi, S. Tiiro, M. López-Benítez, J. J. Lehtomäki, and Y. Suzuki, "Welch FFT segment size selection method for spectrum awareness system," *IEICE Trans. Commun*, vol. E99-B, no. 8, pp. 1813–1823, Aug. 2016.

[20] J. Nikonowicz, A. Mahmood, E. Sisinni, and M. Gidlund, "Noise power estimators in ism radio environments: Performance comparison and enhancement using a novel samples separation technique," *IEEE Trans. Instrum. Meas.*, vol. 68, no. 1, pp. 105–115, Jan. 2019.

[21] M. López-Benítez, J. Lehtomäki, K. Umebayashi, and D. Patel, "Accurate noise floor calibration based on modified expectation maximisation of gaussian mixture," in *Proc. IEEE WCNC*, May 2019.